NANO LETTERS

pubs.acs.org/NanoLett

Letter

Optically Induced Symmetry Breaking Due to Nonequilibrium Steady State Formation in Charge Density Wave Material 1T-$TiSe_2$

Harshvardhan Jog, Luminita Harnagea, Dibyata Rout, Takashi Taniguchi, Kenji Watanabe, Eugene J. Mele, and Ritesh Agarwal*

Cite This: *Nano Lett.* 2023, 23, 9634−9640

Read Online

ACCESS | Metrics & More | Article Recommendations | Supporting Information

ABSTRACT: The strongly correlated charge density wave (CDW) phase of 1T-$TiSe_2$ is of interest to verify the claims of a chiral order parameter. Characterization of the symmetries of 1T-$TiSe_2$ is critical to understand the origin of its intriguing properties. Here we use very low-power, continuous wave laser excitation to probe the symmetries of 1T-$TiSe_2$ by using the circular photogalvanic effect. We observe that the ground state of the CDW phase (D_{3d}) is achiral. However, laser excitation above a threshold intensity transforms 1T-$TiSe_2$ into a nonequilibrium chiral phase (C_3), which changes the electronic correlations in the material. The inherent sensitivity of the photogalvanic technique to structural symmetries provides evidence of the different optically driven phase of 1T-$TiSe_2$, which allows us to assign symmetry groups to these states. Our work demonstrates that optically induced phase change can occur at extremely low optical intensities in strongly correlated materials, providing a pathway to engineer new phases using light.

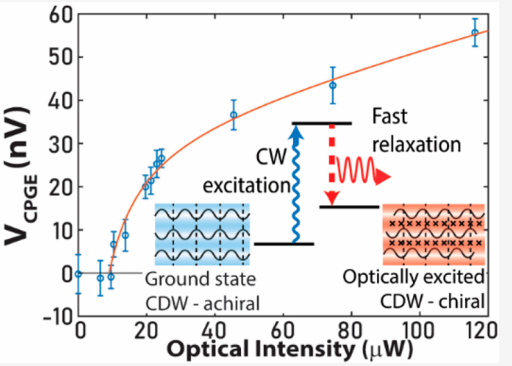

KEYWORDS: *charge density wave, symmetry, photogalvanic effect, 1T-$TiSe_2$*

Probing the structure and symmetries of a material is fundamental to understanding the origins of its physical properties.[1−3] Examining symmetries often becomes complicated by the coupling between the lattice and electronic degrees of freedom, especially in strongly correlated materials.[4−6] In cases where subtle symmetry breaking cannot be easily probed using methods typically used to probe crystal structure such as X-ray or electron diffraction, the measurement has to be indirect, for example by using selection rules for optical probes to infer the underlying symmetries.[7,8] Charge density wave (CDW) systems are one such class of materials with strong correlations between their electronic and structural degrees of freedom. In CDW systems, the electron density forms periodic modulations at wavevectors $\boldsymbol{q}$ which span the Fermi surface and couple with lattice distortions.[9−12] Among these systems, 1T-$TiSe_2$ has been extensively studied with possible excitonic character leading to claims of excitonic insulating behavior at lower temperatures.[13,14] Since the excitonic properties of 1T-$TiSe_2$ are closely related to the structural properties of the CDW phase, it is important to understand the symmetry of the low temperature phase, which can provide a better understanding of the origin of its properties.

1T-$TiSe_2$ is a van der Waals layered transition metal dichalcogenide with layers stacked along the c-axis, where each monolayer is formed by a Ti layer sandwiched between two layers of Se atoms. The high temperature space group is $P\bar{3}m1$ (Figure 1A).[15] 1T-$TiSe_2$ is known to exhibit a $2a_0 \times 2a_0 \times 2c_0$ commensurate CDW transition below ∼200 K into a structure with $P\bar{3}c1$ symmetry.[9,15−17] The CDW transition is also associated with a possible excitonic condensation, associated with a large excitonic binding energy (>50 meV) formed by holes in the valence band composed of two Se 4p orbitals and electrons in the conduction band with one Ti 3d orbital.[13,18]

1T-$TiSe_2$ has an indirect band overlap of the valence and conduction band above T_C, and thus there are three Fermi wavevector orientations $\boldsymbol{q}_F^{1,2,3}$ orientations in the Brillouin zone oriented along the $\overline{\Gamma L}$ directions with a 120° angle between the three wavevectors.[18,19] Since $\boldsymbol{q}_F$ determines the direction of modulation of a CDW, with the existence of three equivalent wavevectors $\boldsymbol{q}_F^{1,2,3}$, there is a possibility of chirality in the CDW phase, where the CDW orientation can wind either clockwise or anticlockwise along the c-axis.[20−22] However, counterclaims of achirality of the CDW ground state in $TiSe_2$ have also been reported.[23,24] Recent experimental studies have suggested that femtosecond optical pulses can transiently change the symmetry of 1T-$TiSe_2$, breaking the CDW coherence, from

Received: September 28, 2023
Revised: October 5, 2023
Published: October 9, 2023

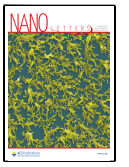

https://doi.org/10.1021/acs.nanolett.3c03736
Nano Lett. 2023, 23, 9634−9640

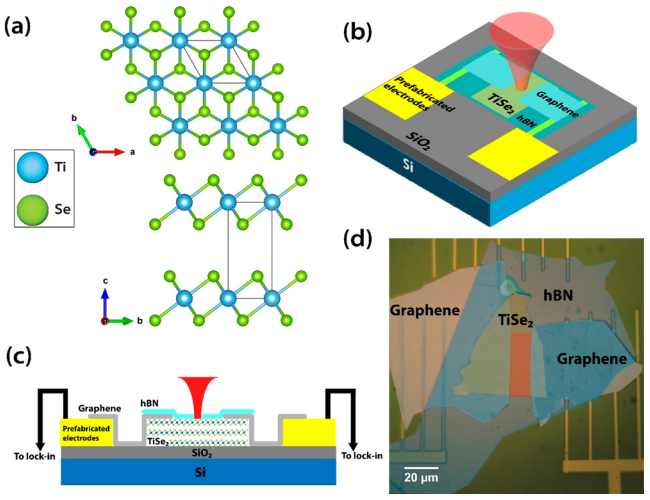

Figure 1. Crystal structure and $TiSe_2$ device architecture used for photocurrent measurements: (a) Crystal structure of 1T-$TiSe_2$ showing the view along the *c*- (top) and *a*-axes (bottom). The material has van der Waals bonding along the *c*-axis, making it quasi-2D in nature. (b) Schematic of a device fabricated for this study. See the Methods section for more details. (c) Cross-sectional schematic of the device architecture. (d) A false color image of a typical device used. The electrodes are multipronged to ensure good contact with graphene flakes. The red shaded region in the center marks the active device area.

the assigned space group $P\bar{3}c1$ below T_C to $P321$.[25,26] However, pump−probe measurement is not very sensitive to the symmetry and chirality of a material as the response depends on the third order permittivity tensor $\chi^{(3)}$, which is nonzero for most systems. $\chi^{(2)}$ has stricter constraints on the allowed elements requiring inversion symmetry breaking and is sensitive to the symmetry of a material. Thus, in order to probe the symmetry of $TiSe_2$, optical probes measuring the $\chi^{(2)}$ response are desirable.

The circular photogalvanic effect (CPGE) measures the $\chi^{(2)}$ response of materials and is sensitive to their symmetries, and unlike second harmonic generation, the experiments can be performed under very weak continuous wave excitation conditions.[27−30] CPGE measures the difference in the DC photocurrents generated by left- and right-circularly polarized light,[27] which can only arise in cases where certain crystalline symmetries are broken. Under the electric-dipole approximation, CPGE is only allowed in systems with broken inversion symmetry, and more specifically only in gyrotropic point groups, i.e., C_1, C_2, C_3, C_4, C_6, C_s, C_{2v}, C_{3v}, C_{4v}, C_{6v}, D_2, D_4, D_{2d}, D_3, D_6, S_4, T, and O.[31] While a crystal having gyrotropic point group symmetry is a necessary condition for observing CPGE, it is not a sufficient condition and depends on the specific experimental geometry, even in the electric-dipole limit.

Here, using CPGE we observe that the ground state of the 1T-$TiSe_2$ CDW phase (below T_C) is achiral and belongs to the point group D_{3d}, but the system transitions into a chiral phase under continuous wave (CW) illumination above a threshold intensity into the point group C_3, indicated by nonzero CPGE. We suggest that this is a result of electronic correlations being suppressed due to an increased free carrier density which screens excitonic correlations in the CDW phase. The change in the local symmetry that we report challenges past studies claiming chirality in the ground state of the CDW phase of $TiSe_2$, and is incompatible with earlier theoretical studies where nonlocal Hall and optical Kerr effects were predicted.[32] Importantly, our work shows that light−matter interactions in correlated phases of matter are complex and can be manipulated to a large degree even under very weak optical excitations.

1T-$TiSe_2$ crystals were grown according to previously reported protocols.[16,33] See Figure S1 for optical images and Figure S2 for the X-ray diffraction data of the as-grown crystal. To measure the photocurrent response of 1T-$TiSe_2$ of freshly cleaved flakes, we used a modified device fabrication process, which involved prefabricating electrodes and placing the $TiSe_2$ flake on them, followed by electrically connecting the flake to the prefabricated electrodes with graphene. The entire device was covered with hBN to protect it from degradation[34] (Figure 1; see Figure S3 and Methods section for details). Figure S4 shows the I−V characteristics of a typical device, which shows Ohmic behavior with minimum or no Schottky barriers. The device was cooled to 140 K inside a cryostat for characterization of the CDW state via CPGE measurements.

For a preliminary symmetry characterization of the $TiSe_2$ flake, linear polarized reflectance of the flake was measured at 140 K. The polarized reflectance data (Figure 2A) shows no change with input light polarization, indicating that the system has crystalline symmetries that do not allow differences between the in-plane ($x-y$ plane) permittivity tensor components. To further test the symmetries of the $TiSe_2$ flake, we measured the polarization dependent photogalvanic response of the device under zero applied bias (see Methods). The incident laser intensity and wavelength were fixed at 100 μW and 600 nm, respectively, unless otherwise specified. The photogalvanic measurement as a function of the angle θ between the quarter waveplate (QWP) with the incident polarization of the laser (Figure 2B) showed that there is a difference in the response at 45° and 135°, which correspond to left-circularly polarized (LCP) and right-circularly polarized (RCP) light, respectively. This indicates the presence of CPGE in the system. The data can be fit to the phenomenological equation for CPGE given by,[27]

$$V_{tot} = V_{CPGE}\sin(2\theta) + V_{LPGE}\sin(4\theta + \delta) + V_0 \quad (1)$$

where V_{tot} gives the total photovoltage (Figure 2B), V_{CPGE} and V_{LPGE} give the circular and linear photogalvanic effect coefficients, respectively, and δ is a phase factor, while V_0 gives the background photocurrent, usually of photothermal and other origins (Supplementary Section 1).

In order to measure the PGE response rapidly and with high resolution, we used a modified fast-rotating QWP setup (see Methods).[35] The laser was maintained at normal incidence to the sample, away from the graphene electrodes to avoid any Schottky effect related response or spatially dispersive CPGE.[29,36] Note that under normal incidence with photovoltage measurement in the $x-y$ plane, only the point groups with no in-plane C_2 symmetry, i.e., C_1, C_{1v}, C_3, C_{3v}, allow nonzero off-diagonal elements in the gyrotropy tensor and can therefore produce CPGE. However, while $TiSe_2$ belongs to the inversion symmetric point group D_{3d}, surprisingly the photoresponse measurement showed a nonzero CPGE signal, indicating the presence of CPGE at normal incidence (Figures 2B). Significantly, no "training" of the $TiSe_2$, i.e., cooling the device while being illuminated with either LCP or RCP light as mentioned in a previous report,[22] was required for the appearance of CPGE (Supplementary Section 2).

https://doi.org/10.1021/acs.nanolett.3c03736
Nano Lett. 2023, 23, 9634−9640

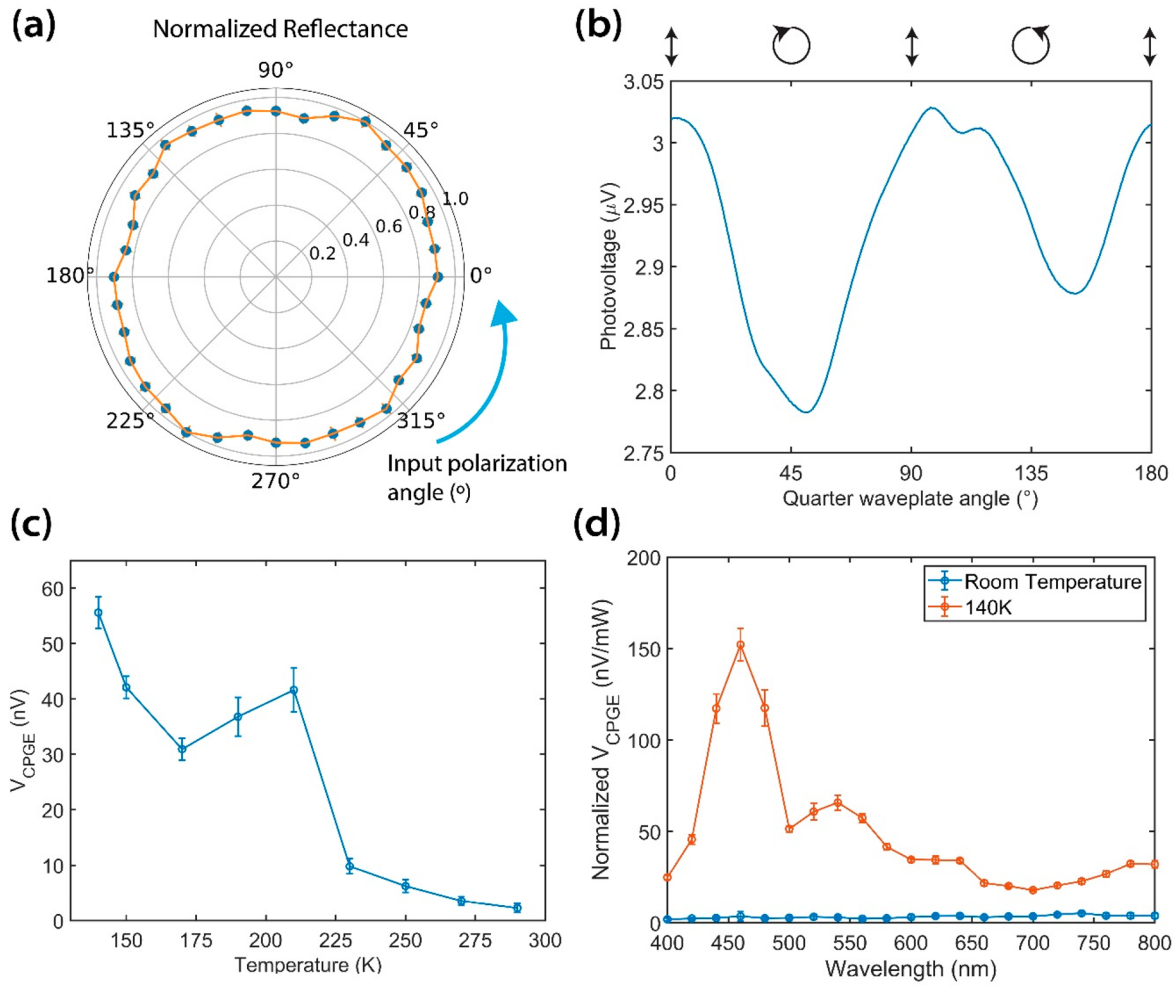

Figure 2. Device characterization using linear and nonlinear photocurrent measurements to probe the symmetry of the CDW phase in $TiSe_2$: (a) Normalized reflectance of $TiSe_2$ from the active device area showing no unique axis in the $x-y$ plane. (b) Typical photoresponse curve of a $TiSe_2$ device as a function of quarter wave-plate angle with the input laser polarization. The device responds differently to left- and right-circularly polarized light, signifying the presence of CPGE. (c) Temperature dependence of V_{CPGE} in a $TiSe_2$ device. The CPGE is nonzero in the low temperature region while it decays sharply above the transition temperature. The dip at ∼175 K is due to an increased resistivity of $TiSe_2$ at that temperature (see Figure S5). (d) Wavelength dependence of V_{CPGE} normalized with input intensity, showing a sharp Lorentzian peak at ∼450 nm and smaller peaks at ∼550 and 650 nm. The room temperature CPGE curve is uniformly zero.

To identify the origin of the CPGE response of the $TiSe_2$ device, we performed temperature-dependent measurements (Figure 2C), which shows nonzero CPGE at low temperatures which drops sharply at 220 K and becomes zero as the temperature increases. This implies that the high temperature phase, where no CDW exists, is not chiral. Note that the T_C of the CDW phase is ∼190−200 K in 1T-$TiSe_2$ (T_C = 195 K for the crystal used here, see Figure S5), but hBN encapsulation can increase the T_C to ∼230 K.[37] Furthermore, the small dip in the CPGE signal at ∼175 K can be explained by noting the same trend in resistivity of 1T-$TiSe_2$ (Figure S5).[38]

To further probe the system, we performed wavelength dependent CPGE measurements normalized with respect to the input laser intensity (Figure 2D). The CPGE spectrum shows a sharp peak at 450 nm with two smaller peaks at ∼550 and 640 nm. Importantly, the Lorentzian line shape of the wavelength dependence indicates a dipolar origin of the CPGE.[30] See Supplementary Section 3 for details about other possible mechanisms for CPGE. However, the observed CPGE in the CDW phase is incompatible with the assigned point group symmetry of $TiSe_2$ (D_{3d}) which forbids CPGE in the dipole approximation due to the presence of inversion symmetry.

In order to resolve the apparent contradiction of the anomalous CPGE observed under CW excitation in our experiments, which is of much lower intensity than pulsed excitation, we measured the laser intensity dependence of the CPGE signal at 600 nm wavelength (Figure 3A). As seen in Figure 3B, we observed three distinct regimes of the CPGE response as a function of the laser input intensity. The low intensity region ($I \leq 10$ μW for the device shown in Figure 3B) shows a nonzero DC photovoltage but no measurable CPGE. At a threshold intensity $I_T \sim 10$ μW, there is a sudden onset of the CPGE response, with the signal rising super-linearly with increasing laser intensity. In the third regime above ∼30 μW, the CPGE showed a linear dependence on the input intensity with a reduced slope. Similar behavior was seen in multiple devices (Figure S6) with different values of I_T depending on slight differences in the device geometry. Also see Figure S7 for piecewise fitting of CPGE with input laser power.

https://doi.org/10.1021/acs.nanolett.3c03736
Nano Lett. 2023, 23, 9634−9640

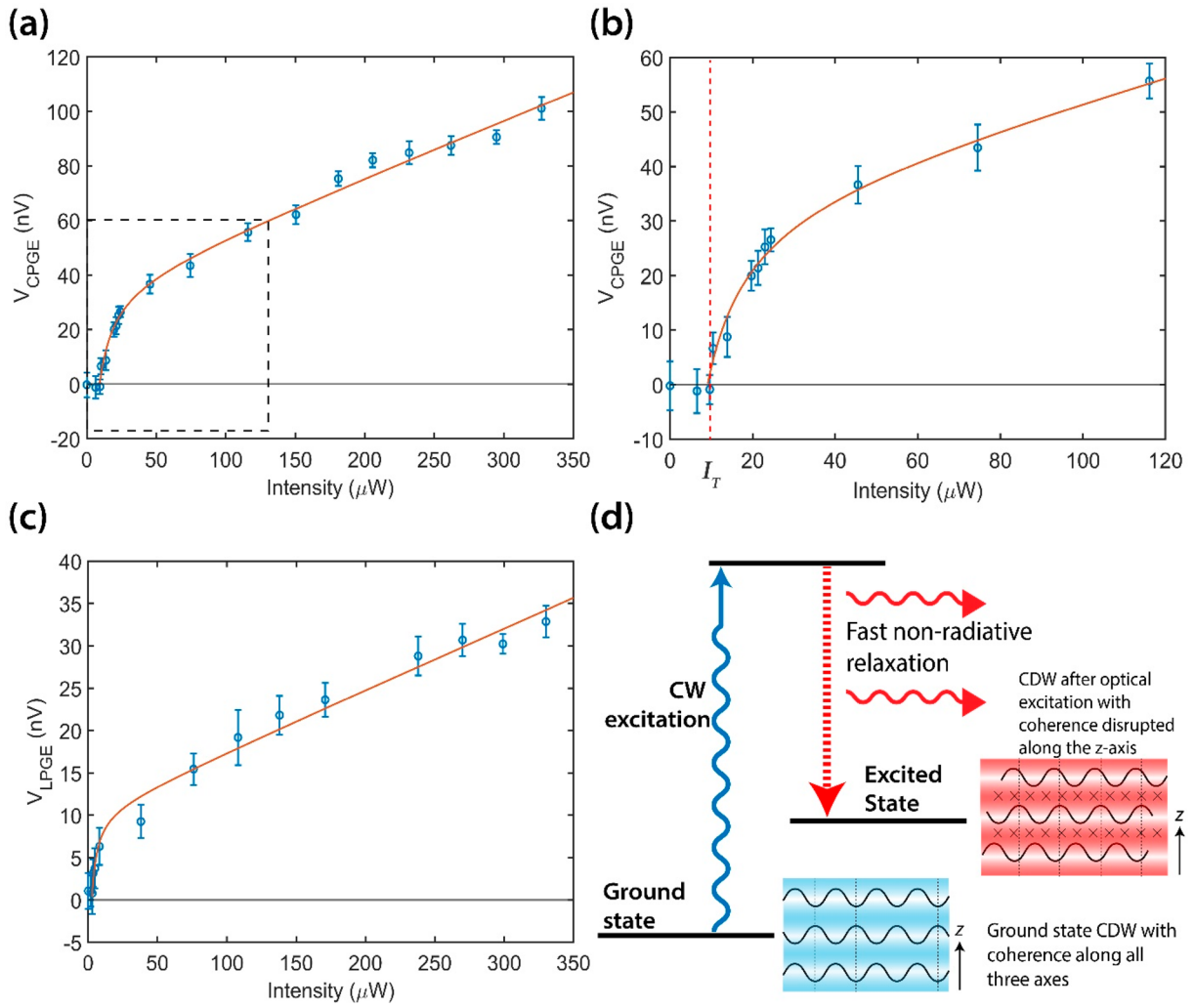

Figure 3. Intensity dependence of the PGE showing nonequilibrium behavior in $TiSe_2$ below T_C. (a) Intensity dependent measurement of CPGE for a typical $TiSe_2$ device. The red line denotes a fit to the nonlinear intensity dependent eq 2 in the main text. (b) Low-intensity region of (a) [the region in the dashed box] zoomed in to show the optically activated nature of CPGE in the system. The observed CPGE is zero up to the threshold intensity $I_T \sim 10$ μW and then sharply increases, and eventually the slope reduces to a stable value. (c) Intensity dependence of LPGE, showing similar optically activated behavior above the threshold intensity. (d) Schematic of a possible process explaining optically triggered behavior. Turning laser illumination on creates a nonequilibrium steady state with free carriers in the conduction band, disrupting the coherence of the CDW in the z-direction, reducing the overall symmetry to C_3.

The linear photogalvanic effect (LPGE) response also requires broken inversion symmetry but has fewer symmetry constraints than CPGE,[39] and shows similar behavior as CPGE with laser intensity (Figure 3C), with a nonzero value in LPGE only appearing for $I > I_T$. Thus, while LPGE would not be allowed in D_{3d} similar to CPGE, the presence of the LPGE response at higher intensities indicates that similar light-induced symmetry breaking processes are governing the presence of CPGE and LPGE in $TiSe_2$.

We summarize our results of the CDW phase in 1T-$TiSe_2$ into four main observations: (1) isotropic reflectance in the linear response at low temperatures, (2) presence of PGE in the low temperature phase but absence of PGE in the high temperature phase, (3) Lorentzian line shape of the wavelength dependence of CPGE, and (4) nonlinear intensity dependence of the CPGE (and LPGE) with threshold behavior. The isotropic nature of the input polarization-dependent reflectance indicates that the combined $TiSe_2$–graphene–hBN system does not have any unique crystallographic axis in the x–y plane, which can potentially arise due to strain or Schottky fields due to electrodes or other factors in the material under study. We can therefore eliminate the point groups C_1, C_i, C_{1v}, C_2, or C_{2v} which would manifest as an anisotropic pattern in the reflectance spectrum due to the presence of two unequal axes in the x–y plane. Hence, consistent with the observation of zero CPGE at low intensities ($I < I_T$), the CDW phase of $TiSe_2$ is assigned a symmetry D_{3d}, since the low intensity white light does not coherently excite carriers to cause disruption to the ground state CDW.

The presence of CPGE under normal incidence of laser at high intensities on the CDW phase of $TiSe_2$ however restricts the possible symmetry of the underlying system to point groups with off-diagonal elements in the gyrotropy tensor γ (Supplementary Section 1). Thus, D_{3d} cannot be the symmetry of the system under higher intensity excitation ($I > I_T$) since the inversion symmetry in D_{3d} prohibits the presence of dipolar CPGE in the system. Moreover, the proposed optically induced point group D_3 as discussed in ref 26 does not explain the CPGE response, since the C_2 symmetry with the rotation axis in the x–y plane forbids any coupling of the

https://doi.org/10.1021/acs.nanolett.3c03736
Nano Lett. 2023, 23, 9634−9640

incident electric fields $E_{x,y}$ with the photoresponse $V_{x,y}^{CPGE}$ being measured in the current device geometry (Supplementary Section 1).

The most important observations are the nonlinearity of the signal with laser intensity and the nonzero threshold intensity I_T for the signal (Figure 3A,B). The system showed no hysteresis upon cycling through high and low intensity laser excitation, indicating that there is a sudden optically induced phase transition in the system at higher-intensity laser excitation, likely of electronic origin. For $I < I_T$, the CDW phase of $TiSe_2$ is in its ground state with the point group D_{3d} which does not support any CPGE or LPGE. However, when the laser intensity is increased to $I > I_T$, optical excitation of $TiSe_2$ above the critical fluence threshold leads to a breakdown of the excitonic correlations and generation of a free carrier density in the conduction band. This affects the coherence between CDWs on different layers along the c-axis due to a transient breakdown of the excitonic correlations formed between the Ti $3d$ orbital and the Se $4p$ orbitals.[25,40] DFT calculations[26] have shown that the ground state CDW of $TiSe_2$ can transiently transform into the space group $P321$ with femtosecond excitations. The space group $P321$ corresponds to the point group D_3 where the C_2 symmetry with the rotation axis in the $x-y$ plane is preserved for a monolayer, setting the $+z$ and $-z$ directions to be equivalent. However, due to the Thomas-Fermi screening from the optically generated free carriers, the CDW is suppressed, and there is no phase correlation between the CDW of any particular layer to that on the top and bottom layers.[25] Thus, the charge densities at a distance of $+z$ are not equivalent to those at $-z$ from any given point of origin, breaking the C_2 symmetry with its rotation axis in the $x-y$ plane. Since the electron densities at $+z$ and $-z$ are now distinct due to the broken symmetry, a net local polarization is formed, and the overall symmetry of the system reduces to C_3 for $I > I_T$. The point group C_3 belongs to the polar point groups and has nonzero off-diagonal elements in the gyrotropic tensor necessary to produce a dipole-order CPGE by coupling the incident in-plane electric fields to the generated photoresponse (Supplementary Section 1).

The nonlinear behavior of the CPGE with laser intensity as well as the requirement of a threshold intensity I_T for a nonzero CPGE response suggests that the change in the local phase to the symmetry broken C_3 phase tracks the free carrier generation and subsequent breakdown of the CDW order along the c-axis (or the z-axis in the lab frame). The observed trend is reminiscent of a three-level system under optical pumping, leading to a free carrier population forming in an excited state under nonequilibrium.[41] When the laser illumination is turned off, the optically excited free carriers quickly relax and the system returns to the inversion symmetric ground state. The process has been schematically summarized in Figure 3D. We can thus model the observed intensity dependence of the CPGE (and LPGE) in Figure 3A−C as a driven three-level system (see Supplementary Section 4):

$$V_{CPGE} = \frac{(1-a)I - 1}{(1+2a)I + 1} b + cI + d \tag{2}$$

where I is the intensity of light and a, b, c, d are fitting parameters. The first term denotes the superlinear increase of CPGE in the low intensity region of the plot, which is similar to what is observed in a three-level system where optical excitation can lead to the formation of a nonequilibrium steady state (NESS) with a quasi-stable free carrier population in the conduction band (CB).[40] The fitting parameter a is related to the ratio of the relaxation times between the higher energy states to CB and from CB to valence band (VB), and the fit in Figure 3A gives a value of $a = 6.6 \times 10^{-8}$ which indicates a fast decay from the excited state to the bottom of the CB (Supplementary Section 4). Such a fast decay is necessary to generate a nonequilibrium population of free carriers for a transient breakdown of the CDW phase. At higher intensities, the equation reduces to $V_{CPGE} \approx cI + d$, implying that after the nonequilibrium steady state is created in the conduction band bottom, further excitation of the system will only increase the CPGE response without further increasing the nonequilibrium free carrier population in the CB. Interestingly, the LPGE is also activated at the same threshold intensity as CPGE (Figure 3C), which implies that the ground state of the CDW before the threshold is symmetric, since the symmetry requirements for nonzero LPGE are more relaxed as compared to those for CPGE.[39] The point group D_{3d} satisfies this requirement, thus confirming that the ground state of the CDW state in $TiSe_2$ is achiral, while C_3 is a polar group allows both CPGE and LPGE, as we observe for $I > I_T$.

In conclusion, carefully designed temperature, wavelength, and intensity dependent CPGE measurements that are very sensitive to the symmetries of the material show that the ground state of the CDW phase in $TiSe_2$ (D_{3d} group) is achiral due to the absence of any CPGE or LPGE at low intensity optical excitation. However, exciting $TiSe_2$ above a threshold laser intensity leads to an optically driven phase transition into a chiral structure with a C_3 point group, triggering CPGE and LPGE response. The effect of light on crystalline symmetry is strong in $TiSe_2$ due to the importance of electron−electron and electron−phonon correlations to the stability of the ground state of the system, and thus, any disruption of these correlations due to free carrier generation leads to a breakdown in the symmetries of the material. Our work thus also sheds light on the role that excitonic correlations play on the symmetries of $TiSe_2$. An important point also to be highlighted is that light can probe and disrupt electronic correlations even at very low intensities and can be utilized to create novel phases of matter.

■ ASSOCIATED CONTENT

Data Availability Statement

All data are available in the main text or the Supporting Information.

Supporting Information

The Supporting Information is available free of charge at https://pubs.acs.org/doi/10.1021/acs.nanolett.3c03736.

Detailed methods (including materials growth and characterization, device fabrication, and measurement techniques), comparison with past literature, consideration of other mechanisms of CPGE, and theoretical results associated with CPGE analysis and nonequilibrium steady state (PDF)

■ AUTHOR INFORMATION

Corresponding Author

Ritesh Agarwal − *Department of Materials Science and Engineering, University of Pennsylvania, Philadelphia, Pennsylvania 19104, United States;* orcid.org/0000-0002-1289-4334; Email: riteshag@seas.upenn.edu

https://doi.org/10.1021/acs.nanolett.3c03736
Nano Lett. 2023, 23, 9634−9640

Authors

Harshvardhan Jog − *Department of Materials Science and Engineering, University of Pennsylvania, Philadelphia, Pennsylvania 19104, United States;* orcid.org/0000-0002-5825-6071

Luminita Harnagea − *Department of Physics, Indian Institute of Science Education and Research Pune, Pune, Maharashtra 411008, India*

Dibyata Rout − *Department of Physics, Indian Institute of Science Education and Research Pune, Pune, Maharashtra 411008, India*

Takashi Taniguchi − *International Center for Materials Nanoarchitectonics, National Institute for Materials Science, Tsukuba 305-0044, Japan;* orcid.org/0000-0002-1467-3105

Kenji Watanabe − *Research Center for Functional Materials, National Institute for Materials Science, Tsukuba 305-0044, Japan;* orcid.org/0000-0003-3701-8119

Eugene J. Mele − *Department of Physics and Astronomy, University of Pennsylvania, Philadelphia, Pennsylvania 19104, United States*

Complete contact information is available at: https://pubs.acs.org/10.1021/acs.nanolett.3c03736

Author Contributions

HJ and RA conceptualized the project. LH and DR synthesized single crystal 1T-$TiSe_2$ and performed XRD and electrical resistivity characterization. TT and KW synthesized hBN. HJ, EJM, and RA formulated the experiments and performed theoretical investigation. HJ fabricated the devices and performed all optoelectronic measurements. EJM and RA acquired funding for the project. HJ and RA drafted the paper, and all authors contributed to reviewing and editing the final draft. RA supervised the project.

Notes

The authors declare no competing financial interest.

■ ACKNOWLEDGMENTS

This work was supported by the US Air Force Office of Scientific Research (award# FA9550-20-1-0345) and the National Science Foundation (NSF-QII-TAQS-#1936276). This work was partially supported by the King Abdullah University of Science & Technology (OSR-2020-CRG9-4374.3) and NSF through the University of Pennsylvania Materials Research Science and Engineering Center (MRSEC) (DMR-1720530) seed grant. Device fabrication and characterization work was carried out in part at the Singh Center for Nanotechnology, which is supported by the NSF National Nanotechnology Coordinated Infrastructure Program under grant NNCI-1542153. L.H. acknowledges financial support from DST-India (DST/WOS-A/PM-83/2021 (G)) and IISER Pune for providing the facilities for crystal growth/characterization. D.R. is thankful for support from IISER Pune. K.W. and T.T. acknowledge support from the JSPS KAKENHI (Grant Numbers 19H05790, 20H00354, and 21H05233).

■ REFERENCES

(1) Kittel, C. Physical Theory of Ferromagnetic Domains. *Rev. Mod. Phys.* **1949**, *21* (4), 541.

(2) Toledano, P.; Toledano, J. *Landau Theory Of Phase Transitions, The Application To Structural, Incommensurate, Magnetic And Liquid Crystal Systems*, 3rd ed.; World Scientific Publishing Company: 1987.

(3) Read, N.; Sachdev, S.; Ye, J. Landau Theory of Quantum Spin Glasses of Rotors and Ising Spins. *Phys. Rev. B* **1995**, *52* (1), 384.

(4) Löhneysen, H. V.; Rosch, A.; Vojta, M.; Wölfle, P. Fermi-Liquid Instabilities at Magnetic Quantum Phase Transitions. *Rev. Mod. Phys.* **2007**, *79* (3), 1015.

(5) Kishimoto, K.; Ishikura, T.; Nakamura, H.; Wakabayashi, Y.; Kimura, T. Antiferroelectric Lattice Distortion Induced by Ferroquadrupolar Order in $DyVO_4$. *Phys. Rev. B* **2010**, *82* (1), No. 012103.

(6) Nakano, A.; Hasegawa, T.; Tamura, S.; Katayama, N.; Tsutsui, S.; Sawa, H. Antiferroelectric Distortion with Anomalous Phonon Softening in the Excitonic Insulator Ta_2NiSe_5. *Phys. Rev. B* **2018**, *98* (4), No. 045139.

(7) Cheong, S. W. SOS: Symmetry-Operational Similarity. *npj Quantum Mater.* **2019**, *4* (1), 1−9.

(8) Zhang, M. Y.; Wang, Z. X.; Li, Y. N.; Shi, L. Y.; Wu, D.; Lin, T.; Zhang, S. J.; Liu, Y. Q.; Liu, Q. M.; Wang, J.; Dong, T.; Wang, N. L. Light-Induced Subpicosecond Lattice Symmetry Switch in $MoTe_2$. *Phys. Rev. X* **2019**, *9* (2), No. 021036.

(9) Wakabayashi, N.; Smith, H. G.; Woo, K. C.; Brown, F. C. Phonons and Charge Density Waves in 1T-$TiSe_2$. *Solid State Commun.* **1978**, *28* (11), 923−926.

(10) Morosan, E.; Natelson, D.; Nevidomskyy, A. H.; Si, Q. Strongly Correlated Materials. *Adv. Mater.* **2012**, *24* (36), 4896−4923.

(11) Van Wezel, J. Chirality and Orbital Order in Charge Density Waves. *EPL (Europhysics Lett.* **2011**, *96* (6), 67011.

(12) Ugeda, M. M.; Bradley, A. J.; Zhang, Y.; Onishi, S.; Chen, Y.; Ruan, W.; Ojeda-Aristizabal, C.; Ryu, H.; Edmonds, M. T.; Tsai, H. Z.; Riss, A.; Mo, S. K.; Lee, D.; Zettl, A.; Hussain, Z.; Shen, Z. X.; Crommie, M. F. Characterization of Collective Ground States in Single-Layer $NbSe_2$. *Nat. Phys.* **2016**, *12* (1), 92−97.

(13) Cercellier, H.; Monney, C.; Clerc, F.; Battaglia, C.; Despont, L.; Garnier, M. G.; Beck, H.; Aebi, P.; Patthey, L.; Berger, H.; Forró, L. Evidence for an Excitonic Insulator Phase in 1T-$TiSe_2$. *Phys. Rev. Lett.* **2007**, *99* (14), No. 146403.

(14) Kogar, A.; Rak, M. S.; Vig, S.; Husain, A. A.; Flicker, F.; Joe, Y. Il; Venema, L.; MacDougall, G. J.; Chiang, T. C.; Fradkin, E.; Van Wezel, J.; Abbamonte, P. Signatures of Exciton Condensation in a Transition Metal Dichalcogenide. *Science.* **2017**, *358* (6368), 1314−1317.

(15) Stirling, W. G.; Dorner, B.; Cheeke, J. D. N.; Revelli, J. Acoustic Phonons in the Transition-Metal Dichalcogenide Layer Compound, $TiSe_2$. *Solid State Commun.* **1976**, *18* (7), 931−933.

(16) Di Salvo, F. J.; Moncton, D. E.; Waszczak, J. V. Electronic Properties and Superlattice Formation in the Semimetal $TiSe_2$. *Phys. Rev. B* **1976**, *14* (10), 4321.

(17) Brown, F. C. Electronic and Vibronic Structure of TiS_2 and $TiSe_2$. *Phys. B+C* **1980**, *99* (1−4), 264−270.

(18) Kidd, T. E.; Miller, T.; Chou, M. Y.; Chiang, T. C. Electron-Hole Coupling and the Charge Density Wave Transition in $TiSe_2$. *Phys. Rev. Lett.* **2002**, *88* (22), No. 226402.

(19) Kaneko, T.; Ohta, Y.; Yunoki, S. Exciton-Phonon Cooperative Mechanism of the Triple- q Charge-Density-Wave and Antiferroelectric Electron Polarization in $TiSe_2$. *Phys. Rev. B* **2018**, *97* (15), No. 155131.

(20) Ishioka, J.; Liu, Y. H.; Shimatake, K.; Kurosawa, T.; Ichimura, K.; Toda, Y.; Oda, M.; Tanda, S. Chiral Charge-Density Waves. *Phys. Rev. Lett.* **2010**, *105* (17), No. 176401.

(21) Castellan, J. P.; Rosenkranz, S.; Osborn, R.; Li, Q.; Gray, K. E.; Luo, X.; Welp, U.; Karapetrov, G.; Ruff, J. P. C.; Van Wezel, J. Chiral Phase Transition in Charge Ordered 1T-$TiSe_2$. *Phys. Rev. Lett.* **2013**, *110* (19), No. 196404.

(22) Xu, S. Y.; Ma, Q.; Gao, Y.; Kogar, A.; Zong, A.; Mier Valdivia, A. M.; Dinh, T. H.; Huang, S. M.; Singh, B.; Hsu, C. H.; Chang, T. R.; Ruff, J. P. C.; Watanabe, K.; Taniguchi, T.; Lin, H.; Karapetrov, G.; Xiao, D.; Jarillo-Herrero, P.; Gedik, N. Spontaneous Gyrotropic Electronic Order in a Transition-Metal Dichalcogenide. *Nature* **2020**, *578* (7796), 545−549.

(23) Novello, A. M.; Hildebrand, B.; Scarfato, A.; Didiot, C.; Monney, G.; Ubaldini, A.; Berger, H.; Bowler, D. R.; Aebi, P.; Renner,

C. Scanning Tunneling Microscopy of the Charge Density Wave in 1T-$TiSe_2$ in the Presence of Single Atom Defects. *Phys. Rev. B* **2015**, *92* (8), No. 081101.
(24) Hildebrand, B.; Jaouen, T.; Mottas, M. L.; Monney, G.; Barreteau, C.; Giannini, E.; Bowler, D. R.; Aebi, P. Local Real-Space View of the Achiral 1T-$TiSe_2$ 2 × 2 × 2 Charge Density Wave. *Phys. Rev. Lett.* **2018**, *120* (13), No. 136404.
(25) Cheng, Y.; Zong, A.; Li, J.; Xia, W.; Duan, S.; Zhao, W.; Li, Y.; Qi, F.; Wu, J.; Zhao, L.; Zhu, P.; Zou, X.; Jiang, T.; Guo, Y.; Yang, L.; Qian, D.; Zhang, W.; Kogar, A.; Zuerch, M. W.; Xiang, D.; Zhang, J. Light-Induced Dimension Crossover Dictated by Excitonic Correlations. *Nat. Commun.* **2022**, *13* (1), 963.
(26) Wickramaratne, D.; Subedi, S.; Torchinsky, D. H.; Karapetrov, G.; Mazin, I. I. Photoinduced Chiral Charge Density Wave in $TiSe_2$. *Phys. Rev. B* **2022**, *105* (5), No. 054102.
(27) Ivchenko, E. L. *Optical Spectroscopy of Semiconductor Nanostructures*; Alpha Science Int'l Ltd.: 2005; pp 361−388.
(28) Ivchenko, E. L.; Ganichev, S. D. *Spin Physics in Semiconductors*; Springer: 2008; pp 281−292.
(29) Dhara, S.; Mele, E. J.; Agarwal, R. Voltage-Tunable Circular Photogalvanic Effect in Silicon Nanowires. *Science.* **2015**, *349* (6249), 726−729.
(30) Jog, H.; Harnagea, L.; Mele, E. J.; Agarwal, R. Exchange Coupling−Mediated Broken Symmetries in Ta_2NiSe_5 Revealed from Quadrupolar Circular Photogalvanic Effect. *Sci. Adv.* **2022**, *8* (7), No. eabl9020.
(31) De Juan, F.; Grushin, A. G.; Morimoto, T.; Moore, J. E. Quantized Circular Photogalvanic Effect in Weyl Semimetals. *Nat. Commun.* **2017**, *8* (1), 15995.
(32) Gradhand, M.; Van Wezel, J. Optical Gyrotropy and the Nonlocal Hall Effect in Chiral Charge-Ordered $TiSe_2$. *Phys. Rev. B* **2015**, *92* (4), No. 041111.
(33) Pistawala, N.; Rout, D.; Saurabh, K.; Bag, R.; Karmakar, K.; Harnagea, L.; Singh, S. Crystal Growth of Quantum Materials: A Review of Selective Materials and Techniques. *Bull. Mater. Sci.* **2022**, *45* (1), 10.
(34) Taniguchi, T.; Watanabe, K. Synthesis of High-Purity Boron Nitride Single Crystals under High Pressure by Using Ba-BN Solvent. *J. Cryst. Growth* **2007**, *303* (2), 525−529.
(35) Ji, Z. *Nonlocal Optoelectronics in Topological Semimetals*; University of Pennsylvania: 2021.
(36) Ji, Z.; Liu, G.; Addison, Z.; Liu, W.; Yu, P.; Gao, H.; Liu, Z.; Rappe, A. M.; Kane, C. L.; Mele, E. J.; Agarwal, R. Spatially Dispersive Circular Photogalvanic Effect in a Weyl Semimetal. *Nat. Mater.* **2019**, *18* (9), 955−962.
(37) Li, L. J.; Zhao, W. J.; Liu, B.; Ren, T. H.; Eda, G.; Loh, K. P. Enhancing Charge-Density-Wave Order in 1T-$TiSe_2$ Nanosheet by Encapsulation with Hexagonal Boron Nitride. *Appl. Phys. Lett.* **2016**, *109* (14), 141902.
(38) Watson, M. D.; Beales, A. M.; King, P. D. C. On the Origin of the Anomalous Peak in the Resistivity of $TiSe_2$. *Phys. Rev. B* **2019**, *99* (19), No. 195142.
(39) Belinicher, V. I.; Sturman, B. I. The Photogalvanic Effect in Media Lacking a Center of Symmetry. *Sov. Phys. Uspekhi* **1980**, *23* (3), 199.
(40) Porer, M.; Leierseder, U.; Ménard, J. M.; Dachraoui, H.; Mouchliadis, L.; Perakis, I. E.; Heinzmann, U.; Demsar, J.; Rossnagel, K.; Huber, R. Non-Thermal Separation of Electronic and Structural Orders in a Persisting Charge Density Wave. *Nat. Mater.* **2014**, *13* (9), 857−861.
(41) Siegman, A. E. *Lasers*; University science books: 1986; pp 248−250.

https://doi.org/10.1021/acs.nanolett.3c03736
Nano Lett. 2023, 23, 9634−9640